Cell Research (2011) 21:183-195.
© 2011 IBCB, SIBS, CAS All rights reserved 1001-0602/11 $ 32.00
www.nature.com/cr

REVIEW

Structural studies of NF-κB signaling

Chao Zheng[1, *], Qian Yin[1, *], Hao Wu[1]

[1]*Department of Biochemistry, Weill Cornell Medical College, New York, NY 10021, USA*

NF-κBs are a family of transcription factors that control a number of essential cellular functions including immune responses, cell proliferation and antiapoptosis. NF-κB activities are tightly regulated through upstream signaling molecules and downstream feedback loops. In this review, structural discoveries in the NF-κB pathway are presented. With the structure information, the following questions may be addressed: (1) How do NF-κBs activate their target genes? (2) How do IκBs inhibit NF-κB activities in the steady state? (3) How do upstream signaling molecules activate the NF-κB pathway? and (4) How do the feedback loops shut down the NF-κB pathway to avoid constitutive NF-κB activation?

***Keywords*:** NF-κB; crystal structure; TRAF; NEMO

Cell Research (2011) **21**:183-195. doi:10.1038/cr.2010.171; published online 7 December 2010

Introduction

NF-κB family proteins are evolutionarily conserved master regulators of immune and inflammatory responses [1, 2]. They play critical roles in a wide array of biological processes including innate and adaptive immunity, embryonic development and oncogenesis. They are activated in response to ligation of many receptors including T-cell receptors, B-cell receptors, members of the tumor necrosis factor (TNF) receptor superfamily and the Toll-like receptor/interleukin-1 receptor (TLR/IL-1R) superfamily. Mammalian, viral and drosophila NF-κB members were coincidently discovered about 25 years ago [3-5], and were soon demonstrated to belong to the same protein family [6-8]. The mammalian NF-κB family consists of p65 (RelA), RelB, c-Rel, p50/p105 (NF-κB1) and p52/p100 (NF-κB2). Today, the study of NF-κB signaling represents a massive collection of effort with over 40 000 publications, dedicated website (www.nf-kB.org) and patents.

NF-κB proteins activate target genes through a highly conserved DNA-binding/dimerization domain called the Rel homology region (RHR) (Figure 1A) [2, 9]. The activities of p65, RelB and c-Rel are tightly regulated by the interaction with inhibitor of κB (IκB). The interaction masks a nuclear localization signal (NLS) and results in the cytoplasmic retention of NF-κB proteins. In comparison, p105 and p100 have an IκB-like domain at their C-terminal region that inhibits the RHR activities *in cis*. Thus, in most cells, NF-κBs are held captive in the cytoplasm from translocating to the nucleus by the IκB proteins or IκB-like domains.

Activation of NF-κB requires phosphorylation of IκB proteins or IκB-like domains, resulting in phosphorylation-induced polyubiquitination via Lys48 of ubiquitins. This polyubiquitination is a signal for degradation of the IκB inhibitor, or processing in the case of p100 or p105, by the proteasome. The freed or processed NF-κB homodimers or heterodimers translocate to the nucleus and recognize specific sequence motifs known as the κB site on their target genes for DNA interaction and transcriptional activation. The κB sites have a great amount of variability. The distinct DNA-binding site specificities of different NF-κB dimers for a collection of related κB sites, and the different protein-protein interactions the individual dimers make at target promoters are some of the reasons for the specificity in NF-κB signaling [2, 9]. In most cases, activation of NF-κB is transient and cyclical in the presence of a continual inducer. These cycles are due to repeated degradation and re-synthesis of IκB and the consequent activation and inactivation of NF-κB, respectively [9].

The Ser/Thr-specific IκB kinases (IKKs) are at the bottleneck for NF-κB activation [10]. A kinase complex, with specificity for the Ser residues in the destruction

*These two authors contributed equally to this work.
Correspondence: Hao Wu
E-mail: haowu@med.cornell.edu

box of IκB, has been known for a long time and was first partially purified from unstimulated HeLa cells. It is now known that the IKK holo-complex contains the kinase, IKKα or IKKβ, and the regulatory protein NEMO (also known as IKKγ or FIP-3) [11-15]. IKK activation is accompanied by phosphorylation of the activation loop

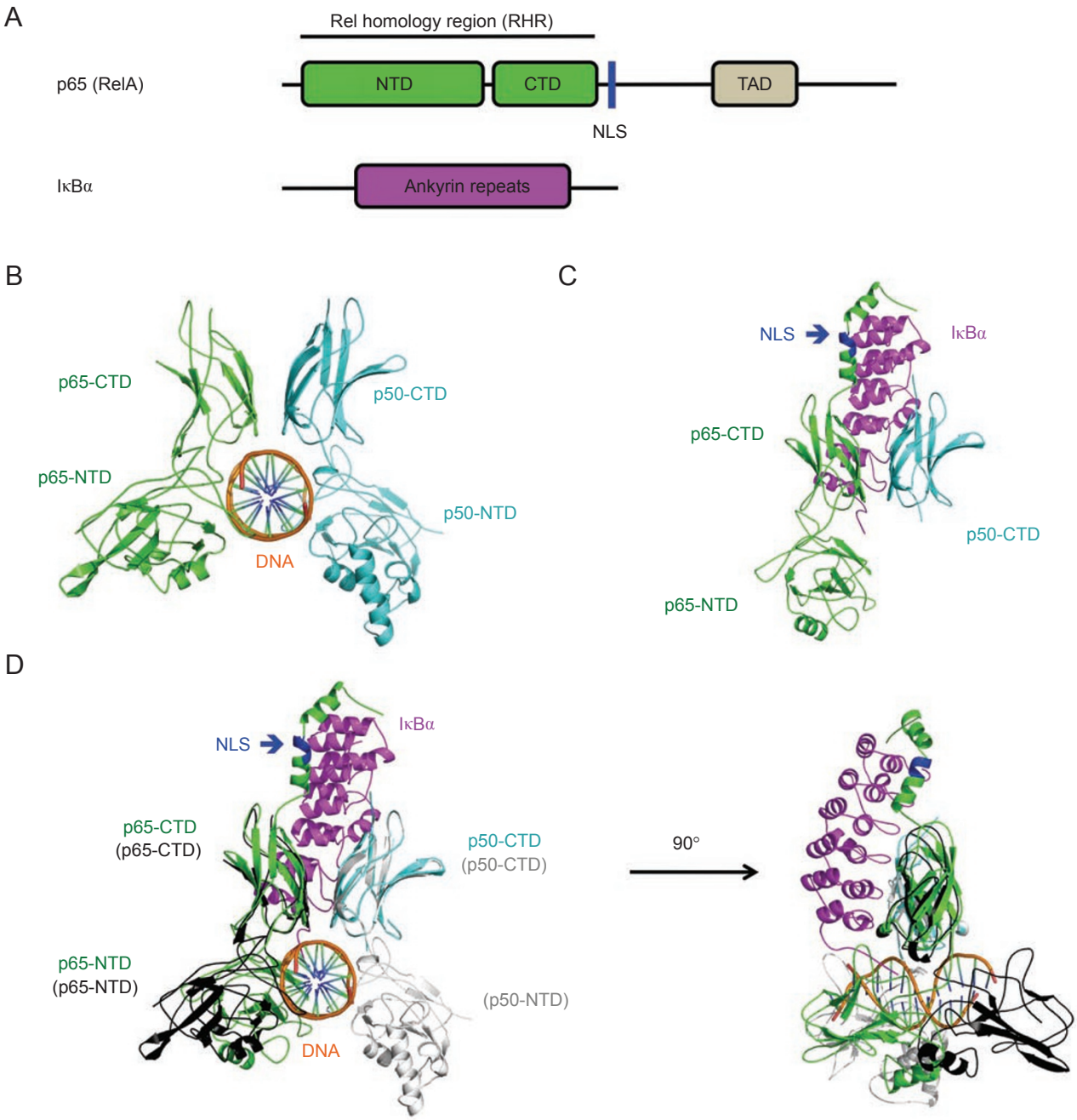

Figure 1 Structures of NF-κB and their complexes with DNA and IκB. **(A)** Domain organization of the NF-κB member p65 and IκBα. NTD: N-terminal domain; CTD: C-terminal domain; TAD: transactivation domain. Location of the nuclear localization signal (NLS) of p65 is shown. **(B)** Structure of the p65/p50 heterodimer:DNA complex (PDB:1VKX). **(C)** Structure of the p65/p50 heterodimer:IκBα complex (PDB:1NFI). Upon interacting with IκBα (magenta), the NLS (blue) of p65 (green) adopts a helical conformation. The p50 subunit (cyan) used to crystallize the complex contains only CTD. **(D)** Superimposition of the p65/p50 heterodimer in complex either with DNA or IκBα. The p65 and p50 subunits in complex with DNA are shown in black and gray, respectively. Upon interacting with IκBα, the NTD of p65 undergoes large conformational changes that prevent DNA interaction.

Ser residues in the canonical MEK (MAP kinase kinase) consensus motif SxxxS in the kinase domain [11-16]. NEMO is critical for IKK activation because in cells lacking NEMO, IKKα and IKKβ cannot be activated by any of the classical NF-κB inducers [15]. While IKKβ is responsible for activation of the canonical NF-κB pathway in response to pro-inflammatory stimuli [17, 18], IKKα plays an indispensable role in the non-canonical NF-κB pathway by phosphorylating p100, leading to its processing and nuclear translocation [19, 20].

Receptor-induced IKK activation pathways have been elucidated for both the TNF receptor superfamily and the TLR/IL-1R superfamily. Upon TNFα binding, TNFR1 recruits the adaptor protein TRADD through death-domain interactions, which in turn recruits TRAF2. Many other TNF receptor superfamily members such as CD40 directly recruit TRAF family members including both TRAF2 and TRAF6. Activation of the TLR/IL-1R superfamily members leads to recruitment of TIR domain-containing adaptors such as MyD88 via TIR domain interactions, which in turn recruits IRAK proteins via death-domain interactions. IRAK proteins are then able to directly interact with and activate TRAF6.

IKK activation in these signaling pathways has been shown to depend on Lys63-linked non-degradative polyubiquitination [21]. For the IL-1R and TLR signaling pathways, TRAF6 acts as the ubiquitin ligase (E3) to mediate Lys63-linked polyubiquitination of itself and downstream proteins such as IRAK1, in conjunction with the specific dimeric ubiquitin conjugating enzyme Ubc13/Uev1A complex (E2). For the TNFα signaling pathway, the RIP1 kinase is Lys63-polyubiquitinated by the TRAF2:cIAP1/2 complex [22-25]. In TNF-mediated IKK activation pathways, TRAF2 and cIAP1/2 are also critical components of the E3 complex that regulates the stability of NIK, a kinase that phosphorylates IKKα and activates NF-κB via the non-canonical NF-κB signaling pathway [26-31]. Deubiquitinating enzymes such as A20 and CYLD downregulate the pathway in the negative feedback loops.

Increasing evidence suggests that NF-κB signaling pathways play important roles in both inflammation and tumor development [1, 32-41]. In fact, it has been shown that inflammation and tumorigenesis are highly linked processes [1, 33]. NF-κB inducible genes include inflammatory and immunoregulatory genes, anti-apoptotic genes and genes that positively regulate the cell cycle. Chronic inflammation prevents elimination of genetically altered cells and enhances metastatic potential. Constitutive NF-κB activities are found in a large number of inflammatory diseases and malignancies including epithelial and lymphoid tumors. Because of the importance of the NF-κB pathway in human diseases, many key signaling proteins in this pathway have become potential therapeutic targets. In this review, we highlight the structural studies in NF-κB signaling pathways in the following five sections.

NF-κB: the central transcription factor

DNA recognition by NF-κB

The RHR of NF-κB proteins is responsible for dimerization, DNA binding, nuclear localization and IκB binding [42-44]. The structure of p50 bound to a palindromic κB site first showed that RHR contains two immunoglobulin-like domains connected by a short flexible linker and interacts with DNA in the major groove [45, 46]. A number of additional structures of RHR homo- and heterodimers bound to DNA targets have confirmed a common mode of dimerization and DNA recognition [45-49] (Figure 1B). The N-terminal domain (NTD) interacts with DNA bases specifically and phosphate backbones nonspecifically. The C-terminal domain (CTD) mediates dimerization and nonspecific DNA contacts. Instead of using α-helices to interact with DNA, as often seen in other transcription factors, NF-κB dimers use flexible loops from the NTD and CTD to mediate DNA contacts. The consensus sequence of NF-κB target genes is 5′-GGGRNYYYCC-3′ (where R is a purine, Y is a pyrimidine and N is any nucleotide), which consists of two half sites [44]. Different NF-κB members prefer different half sites. For example, p50 recognizes a five base pair half site, whereas p65 uses a four base pair half site. In certain cases, the presence of one half site is sufficient for the recruitment of an NF-κB dimer [48]. C-terminal to the RHR is a flexible region that contains the nuclear localization signal.

Interaction of NF-κB with its inhibitor IκB

IκB can be categorized into classical IκB (IκBα, IκBβ and IκBε), NF-κB precursors (p105 and p100) and nuclear IκB (IκBζ, Bcl-3 and IκBNS) [50]. All the IκB family members contain a conserved central ankyrin repeat domain (ARD) that is responsible for interacting with NF-κB (Figure 1A). Each subfamily of IκB has its own preferred NF-κB binding partners. The classical IκBs bind NF-κB dimer with at least one p65 or c-Rel subunit, the non-classical IκBs are able to bind all NF-κB subunits and the nuclear IκBs have specificities for p50 or p52 homodimer [50, 51]. The crystal structures of the IκBα:NF-κB p50/p65 heterodimer complex (Figure 1C) [52, 53] and IκBβ:NF-κB p65/65 homodimer [54] have been solved. In these structures, each NF-κB dimer binds to one molecule of IκB. The ARDs of IκBα

and IκBβ consist of six ankyrin repeats stacking together forming an elongated structure. Each layer is an ankyrin repeat that contains an outer helix, an inner helix and a short β-hairpin. In both complexes, ankyrin repeats 1 and 2 contact the NLS-containing C-terminal region of one p65 subunit. Ankyrin repeats 4, 5 and 6 interact with the RHR-CTD of NF-κB. While the IκBβ:NF-κB complex is still able to bind to DNA, the presence of IκBα inhibits the DNA-binding ability of NF-κB. In the IκBα:NF-κB complex, ankyrin repeat six and the C-terminal PEST residues interact with the p65 RHR-NTD, occupying the DNA-binding residues of NF-κB. In addition, upon interacting with IκBα, p65 subunit undergoes a large conformational change locking NF-κB into a closed conformation [52, 53] (Figure 1D). In contrast, it appears that the NTD of the p65 homodimer do not contact IκBβ and are free to bind DNA even in the presence of IκBβ [54].

NEMO: the key IKK regulatory subunit

Recognition of IKKβ by NEMO

NEMO, the regulatory component of the IKK complex, appears to be a highly helical protein with an N-terminal kinase-binding domain (KBD) that includes a helical domain (HLX1) and part of coiled-coil domain 1 (CC1), a second helical domain (HLX2), another coiled-coil domain CC2, a leucine zipper domain (LZ) and a zinc-finger (ZF) domain [15, 55, 56] (Figure 2A). The crystal structure of the complex between NEMO KBD and the IKKβ C-terminal region shows a heterotetramer with two molecules from each protein [57] (Figure 2B). The four molecules pack as a parallel four-helix bundle. NEMO molecules are each a crescent-like α-helix, and interact with each other at both N- and C-termini, leaving an open slit in the middle. The more extensive N-terminal interface comprises both hydrophobic and charge interactions, while hydrophobic interaction alone contributes to the C-terminal dimer interface. Overall, the NEMO dimer is symmetrical. The only subtle exception is for some C-terminal interfacial residues that adopt different side chain conformations to make distinct contacts with IKKβ. The two IKKβ peptides do not interact with each other, but are associated with both NEMO molecules. The consensus NEMO-binding site of both IKKα and IKKβ contains a LDWSWL sequence [58, 59]. Bulky side chains such as the Trp residues in the consensus sequence fit nicely into nonpolar pockets created by both strands of NEMO to attain specificity.

NEMO and Kaposi's sarcoma herpesvirus FLIP (ks-vFLIP)

Since NEMO is absolutely required for canonical NF-κB activation, it is not surprising that it falls prey to certain viruses. ks-vFLIP is one such usurper. Bagneris *et al*. reported the crystal structure of NEMO (150-272) in complex with ks-vFLIP [60] (Figure 2C). The construct used for crystallization spans from the C-terminal region of CC1 to the N-terminal region of CC2. However, only the region between CC1 and CC2 (193-253) is visible in the structure, which is dubbed the HLX2 domain. The structure consists of a central HLX2 coiled-coil dimer and two symmetrically bound ks-vFLIPs. The two ks-vFLIP molecules clamp the C-terminal half of HLX2. Of the ks-vFLIP tandem death-effector domains (DEDs), the NEMO coiled coil fits snugly into two clefts on the surface of the first DED domain. While both clefts are key to the interaction, the interaction in the first cleft is more extensive, with hydrophobic contacts in the upper compartment and more hydrophilic interactions in the lower compartment. It is postulated that stabilization of NEMO dimerization, either by ks-vFLIP or receptor signaling, activates NEMO and NF-κB. L227P, a NEMO mutation found in patients with anhidrotic ectodermal dysplasia with immunodeficiency may change the helical tendency of NEMO and destabilize the NEMO dimer [60].

Diubiquitin interaction by NEMO

The CC2-LZ region of NEMO interacts with ubiquitin and its crystal structures, both alone and in complex with linear or Lys63-linked diubiquitin (di-Ub), have been determined [61-63] (Figure 2D). In all cases, NEMO CC2-LZ forms a parallel dimeric coiled coil expanding about 100 Å in length. Interestingly, the dimer does not strictly observe two-fold symmetry. A Pro residue (P299 in human NEMO and P292 in mouse NEMO) between CC2 and LZ breaks the otherwise continuous α-helix and provides a "hinge" as the natural boundary between the two domains. Unlike classical coiled coils, where the *a* and *d* positions of the heptad repeats are occupied by hydrophobic residues, CC2-LZ dimer packs against each other using both hydrophobic residues and aliphatic portions of charged residues. CC2-LZ preferentially binds linear di-Ub, has a modest affinity towards Lys63-linked di-Ub, but does not bind Lys48-linked di-Ub at all. Structural and biochemical studies showed that the ubiquitin-binding motif resides in the LZ domain, right after the "hinge". The ubiquitin-binding surface is composite, with contributions from both NEMO molecules. In linear di-Ub binding, NEMO binds to the conserved hydrophobic patch and the C-terminal tail of distal ubiquitin and recognizes an adjacent surface on proximal ubiquitin [61]. The stoichiometry between NEMO and di-Ub is debatable, as both 2:2 and 2:1 have been observed [61, 62, 64]. It is possible that NEMO contains a high-affinity

ubiquitin-binding site for the distal ubiquitin in both linear and Lys63-linked di-Ub. For linear di-Ub, the proximal ubiquitin contacts the same NEMO dimer, creating high affinity in the interaction. For Lys63-linked di-Ub, only one ubiquitin contacts each NEMO dimer, explaining the much lower affinity between NEMO and Lys63-linked di-Ub [62].

NEMO zinc finger

Zinc finger (ZF) constitutes the extreme C-terminal end of NEMO. NMR studies of NEMO ZF and its C417F mutant revealed a canonical β-β-α fold [63, 64] (Figure 2E). Interestingly, replacement of the last Cys residue with a non-chelating Phe did not disrupt its ZF fold or its zinc ion chelating ability, although the Phe residue swings away from the zinc site and shortens the α-helix by half a pitch. Analysis of NEMO ZF surface suggests protein:protein interaction potentials. NMR studies showed that the NEMO ZF is a ubiquitin-binding domain (UBD). It binds to ubiquitin in a 1:1 fashion with submillimolar affinity. The amphipathic α-helix in ZF interacts with the I44-centered hydrophobic patch of ubiquitin, reminiscent of the interactions between α-helical UBDs and ubiquitin.

Full-length NEMO

Structures of domains of NEMO enable a likely view of activated, full-length NEMO as an elongated, flexible

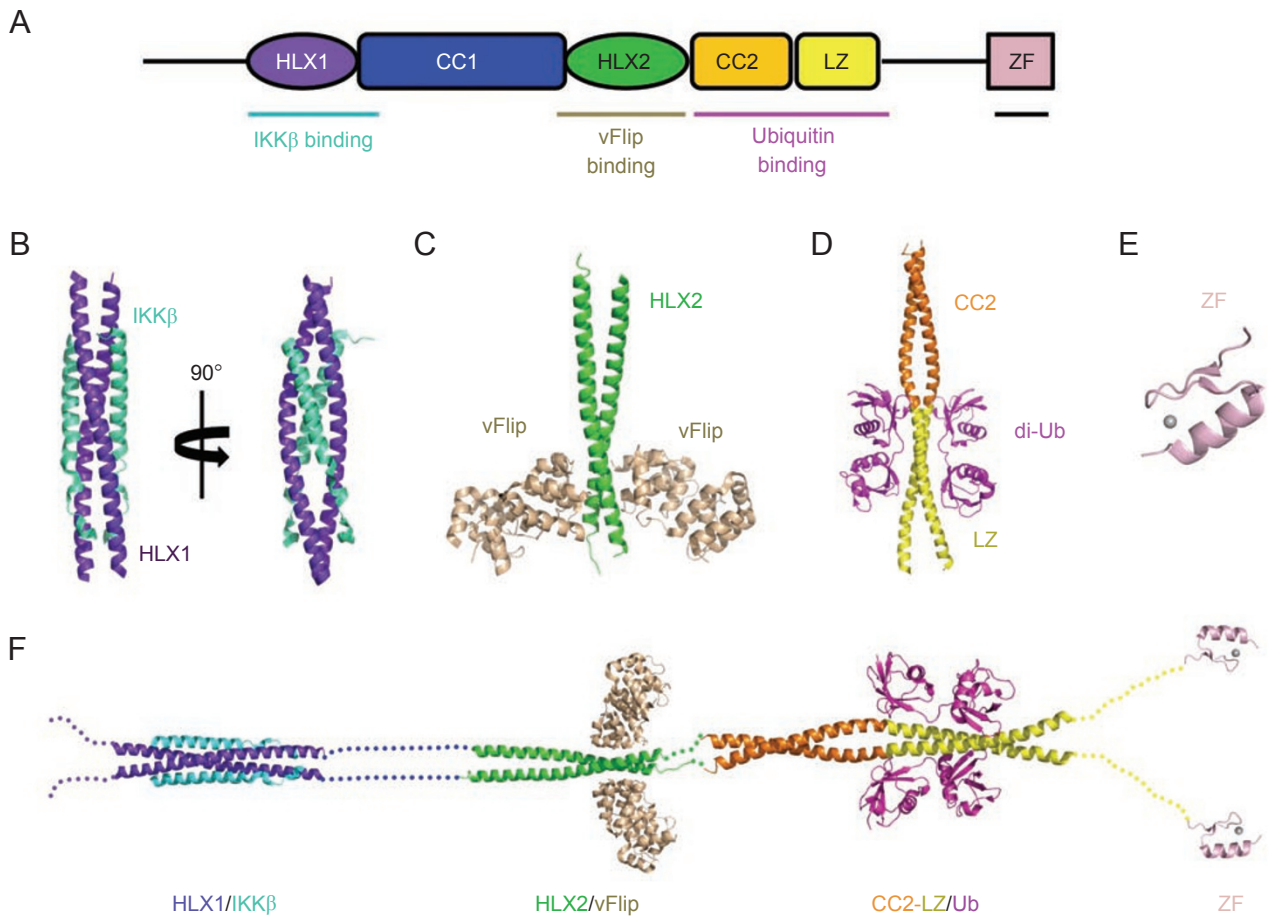

Figure 2 Structures of NEMO and their complexes. **(A)** Domain organization of human NEMO. Solid bars below the diagram indicate current NEMO structures and their binding partners. HLX: helical domain; CC: coiled coil; LZ: leucine zipper; ZF: zinc finger. **(B)** Structure of NEMO KBD in complex with an IKKβ peptide (PDB code 3BRT). Two orthogonal views show the central slit in NEMO dimer and the binding mode of the IKKβ peptide. **(C)** Structure of NEMO HLX2 (green) in complex with ks-vFlip (wheat) (PDB code 3CL3). **(D)** Structure of mouse NEMO CC2-LZ domain in complex with linear di-Ub (PDB code 2ZVN). **(E)** Structure of NEMO zinc finger (PDB code 2JVX). The zinc ion is shown as a gray sphere. **(F)** Proposed model of full-length NEMO as an elongated dimer. All structurally determined domains are colored as in **(A-E)**; regions without known structures are shown as dotted lines.

dimeric coiled coil (Figure 2F).

TRAFs: major adaptor and ubiquitin ligase

TRAF trimerization and interaction with receptors and adaptor proteins

TNF and related ligands are trimeric in nature. Upon ligand binding, TNFRs assemble into specific trimeric complexes [65] that recruit intracellular TRAFs [66, 67]. Depending on the receptors, TRAFs can be recruited to these receptors either via direct interactions or via intermediary adapter proteins such as TRADD and IRAK. TRAF proteins contain an N-terminal region with RING and zinc-finger domains and a C-terminal region with coiled coil and TRAF-C domains (Figure 3A). The TRAF-C domain mediates interactions with receptors and adaptor proteins, and is responsible for the specificity and diversity of TRAF recruitment. Structures of TRAF2 in complex with receptor peptides and TRADD have been reported, revealing a shallow surface on TRAF2 for these interactions [66-73] (Figure 3B and 3C). Structures of TRAF6 in complex with receptor peptides showed an analogous surface groove that possesses distinct receptor-interaction specificity [69].

TRAF RING and ZF structures and interaction with Ubc13

The N-terminal region of TRAF proteins may function as a ubiquitin ligase (E3) for Lys63-linked polyubiquitination. Structure of TRAF6 showed that the RING and following three ZFs are arranged linearly in a rigid golf club-like conformation (Figure 3D), rather than "beads-on-a-string" [74]. The RING domain conforms to the canonical "cross-brace" fold but with the last zinc-coordinating residue replaced by an Asp. All three ZFs in TRAF6 structure share the canonical β-β-α structure and exhibit a conserved orientational relationship between them. Hence additional ZFs in TRAF6 can be modeled to generate the full-length structure of TRAF6.

The interaction between TRAF6 and its cognate E2 Ubc13 (Figure 3E) is similar to other RING/E2 interactions. In the core of this interaction are hydrophobic contacts from the RING domain near the first zinc-binding site. Residues preceding the RING enhance the interaction by providing additional charge:charge contacts. This additional interaction may account for the relatively high affinity between TRAF6 and Ubc13. The first ZF does not directly interact with Ubc13 but is required for this interaction. It forms a three-stranded anti-parallel β-sheet with residues that precede the RING, locking them into the interaction-facilitating conformation. It has long been assumed that like TRAF6, TRAF2 functions as an E3 to add Lys63-linked polyubiquitin chains to itself and other substrates. Unexpectedly, superposition of TRAF2 N-terminus structure onto TRAF6/Ubc13 structure reveals two regions of clashes, hence, precluding TRAF2/Ubc13 interaction [75] (Figure 3F). Consistently, purified N-terminal construct of TRAF2 does not interact with Ubc13 in gel-shift assay under the same condition where N-terminal construct of TRAF6 shows a robust shift. This incapability of interaction might not be limited to Ubc13, as modeling shows similar clashes with UbcH5b. In addition, TRAF6 residues critical for Ubc13 interaction are not conserved in TRAF2. Mutation of these residues to their TRAF2 counterparts abolishes Ubc13 interaction and E3 activity of TRAF6 [74]. This new evidence prompts a re-evaluation of TRAF2 function in TNF receptor signaling.

Symmetry mismatch and higher-order aggregation

The N-terminal regions of both TRAF2 and TRAF6 are dimers in crystal lattices and in solution [74, 75] (Figure 3D and 3G). The RING domain and the following linker region both participate in dimer formation. Aromatic and aliphatic side chain stacking forms the mainly hydrophobic dimer interface. Dimerization is critical for TRAF6 E3 activity *in vitro* and NF-κB activation *in vivo*, as dimerization defective mutants are compromised in polyubiquitin chain assembly and the ability to promote IκB phosphorylation [74]. The dimerization residues are well conserved among TRAF family members, which underlines the importance of dimerization.

Given that the C-terminal regions of TRAF proteins are trimeric, symmetry mismatch exists between the N- and the C-terminal regions. Our fluorescence resonance energy transfer (FRET) experiments showed that TRAF6 is capable of higher-order oligomerization, which can be disrupted by an N-terminal region dimerization mutation [74]. In addition, spontaneous TRAF6 aggregation occurs upon receptor stimulation under endogenous conditions, forming microscopically discernable clusters on the cell surface [74]. The observed higher-order aggregation of TRAF6 is consistent with an infinitely expandable model of full-length TRAF6 in its activated state as a consequence of the symmetry mismatch (Figure 3H). The massive increase in local concentrations of the associated signaling proteins in this aggregation platform probably acts as a factory to promote polyubiquitin synthesis, autoubiquitination and recruitment of downstream proteins to facilitate signal transduction.

Recognition of cIAP1/2 by TRAF2 trimer and the TRAF1:TRAF2 heterotrimer

TRAF2 and cIAP1/2 form an E3 complex that plays

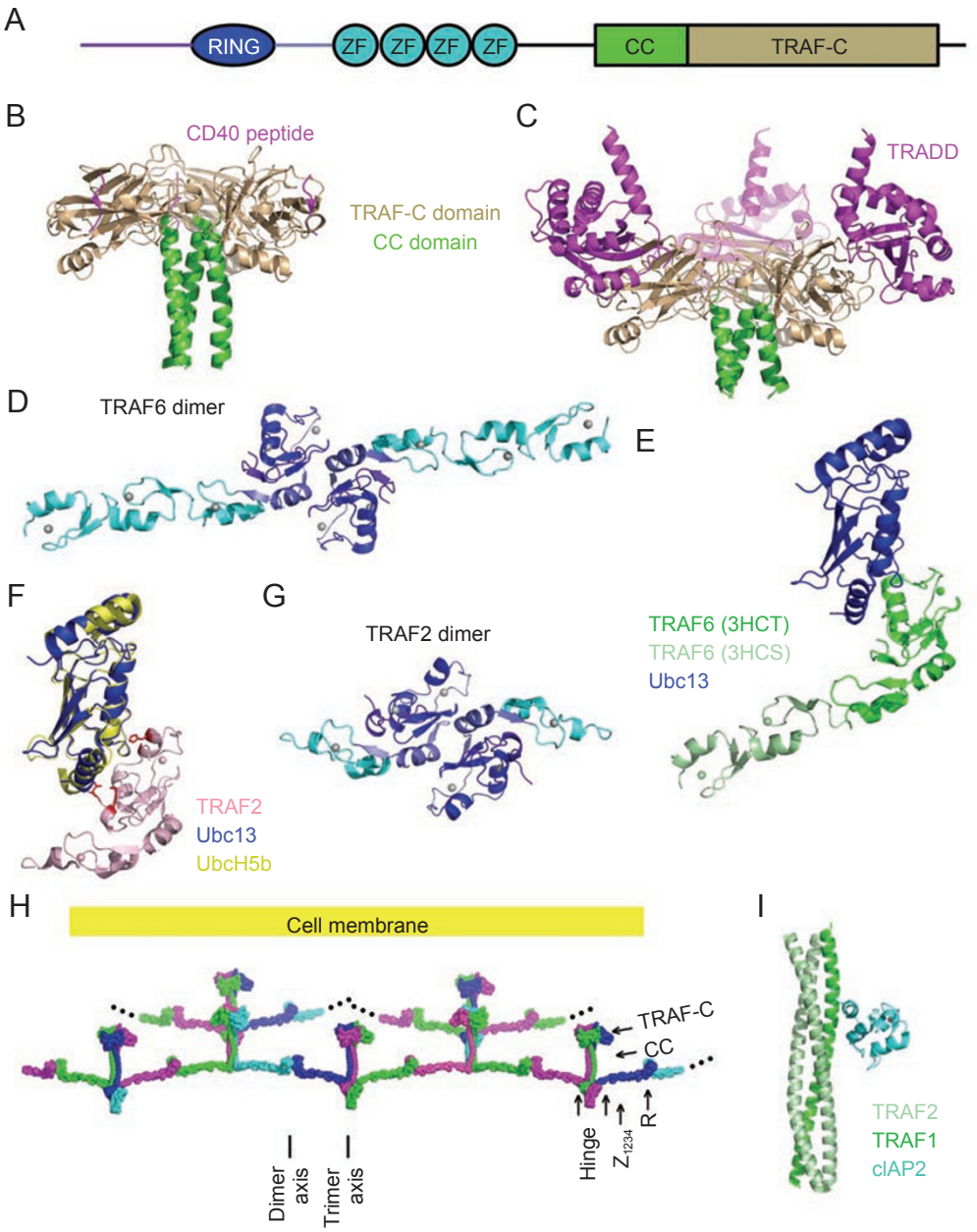

Figure 3 Structures of TRAF and their complexes. **(A)** The common domain organization of TRAF2 and TRAF6. **(B)** Structure of TRAF2 C-terminal region in complex with human CD40 peptide (PDB ID 1QSC). Magenta: CD40. **(C)** Structure of TRAF2 C-terminal region in complex with TRADD (PDB ID 1F3V). **(D)** Structure of TRAF6 N-terminal region dimer (PDB code 3HCS). Domains/motifs are colored according to the scheme in **(A)**. Zinc ions are shown as gray spheres. **(E)** Structure of TRAF6 N-terminal region in complex with Ubc13 (PDB code 3HCT). Green: TRAF6; blue: Ubc13. The second and third zinc fingers (in pale green) are appended to the C-terminal end of TRAF6 in 3HCT based on structure superposition. Zinc ions are shown as spheres, colored in green or pale green, accordingly. **(F)** Structure model showing clashes between TRAF2 and Ubc13 or UbcH5b. TRAF2 (PDB ID 3KNV) and UbcH5b (PDB ID 2CLW) are superimposed onto TRAF6/Ubc13 complex (PDB ID 3HCT), respectively. For clarity, TRAF6 molecule is removed. Pink: TRAF2; blue: Ubc13; yellow: UbcH5b. Side chains causing clashes are shown as sticks and colored in red. **(G)** Structure of TRAF2 dimer (PDB ID 3KNV). Structure elements are colored the same as TRAF6 in **(D)**. **(H)** A model of oligomerized full-length TRAF6 in the activated state, showing the potential for infinite aggregation. TRAF6 is shown in four alternative colors (magenta, green, cyan and blue) and is modeled by piecing together the N-terminal region structure and the C-terminal region structure. Zinc finger 4 is modeled based on its predicted relationship with zinc finger 3. The linker between zinc finger 4 and the coiled coil may act as a flexible hinge. R: RING. **(I)** Structure of TRAF1-CC:TRAF2-CC:cIAP2 (right, PDB ID 3M0D) complex. Zinc ions are shown as gray spheres.

important roles in canonical and non-canonical NF-κB pathways, as well as in the development of MALT B-cell lymphoma. The crystal structure of the TRAF2:cIAP2 complex [76] showed that the coiled-coil region of TRAF2 forms a homotrimer and interacts with one molecule of cIAP2 BIR1 domain, a stoichiometry that was confirmed by multiple techniques and by another group [77]. TRAF2 alone adopts a symmetrical trimer conformation, whereas the TRAF2 trimer in the TRAF2:cIAP2 complex is somewhat asymmetrical. Hence, it seems that, upon interacting with one molecule of cIAP2, TRAF2 undergoes a conformational change that prevents additional cIAP2 molecules from binding to the TRAF2 trimer. Two chains of the TRAF2 trimer directly contact cIAP2 with one chain providing more contacts than the other.

Although it is known that TRAF1 and TRAF2 interact with each other, we unexpectedly showed that they form a distinct TRAF1:$(TRAF2)_2$ heterotrimeric complex [76]. Subsequent biochemical characterization showed that the heterotrimeric complex interacts with cIAP2 with highest affinity, followed by the TRAF2 trimer, while the TRAF1 trimer interacts very weakly with cIAP2. The crystal structure of the TRAF1:$(TRAF2)_2$:cIAP2 complex (Figure 3I) is similar to that of the TRAF2:cIAP2 complex. Surprisingly, it is TRAF1 that mediates most of the interaction with cIAP2, an interaction that appears to exhibit higher shape complementarity and hydrophobicity. cIAP1 and cIAP2 share 73% sequence identify and have redundant functions [22, 78]. Therefore, cIAP1 is expected to bind to TRAF1/2 in a similar fashion as cIAP2.

NF-κB activation by Toll-like receptors: the MyD88:IRAK4:IRAK2 complex

The TLR intracellular signal transducer MyD88 and the IRAK kinases are crucial for anti-pathogen responses and inflammation. We recently showed that MyD88, IRAK4 and IRAK2 assemble into a tertiary complex through their death domains (DD) (Figure 4A) [79]. The crystal structure of the complex revealed a helical oligomer with six MyD88, four IRAK4 and four IRAK2 DDs that form a tower-shaped structure (Figure 4B). The DD helix contains approximately 3.7 DD molecules per turn with 4 DD molecules forming a layer of the helix. Assembly of the helical oligomer is likely to be hierarchical and explains the sequence of events in TLR signaling. MyD88 oligomerization first results in IRAK4 recruitment and activation of the IRAK4 kinase domain through induced proximity. The subsequent recruitment of IRAK2 or IRAK1 allows IRAK4 to phosphorylate these IRAKs. Hyperphosphorylated IRAK1 or IRAK2 then leaves the complex to interact with TRAF6 for IKK activation. Unexpectedly, despite the different overall architecture, the interactions in the complex are similar to DD complexes in cell death signaling [82-84].

Deubiquitinases: the negative regulators

Non-destructive polyubiquitin chains play important roles in NF-κB activation pathways by serving as scaffolds for recruitment of signaling proteins [21]. One way of terminating the NF-κB pathway is to remove the non-destructive polyubiquitin chains that are required for the activation stage by deubiquitinases (DUBs). Constitutive activation of the NF-κB pathway is often associated with aggressive tumor formation and cancer therapy resistance in patients [80, 81]. Two DUBs, A20 and CYLD, are important in this negative feedback regulation of NF-κB activation [82-86].

A20

A20 is a member of the ovarian tumor (OTU) superfamily of DUBs [87]. It has an OTU domain at the N-terminal region and seven ZF motifs at the C-terminal region (Figure 5A). The A20 OTU mediates deubiquitination of Lys63-linked polyubiquitin chain. However, the fourth A20 ZF motif also has E3 ligase activity that generates Lys48-linked polyubiquitin chains. Both the deubiquitination and ubiquitination activities of A20 are required for NF-κB inhibition, making A20 a ubiquitin-editing enzyme [88, 89].

The crystal structures of A20 OTU domain [90, 91] revealed a teakettle-shaped molecule (Figure 5B) with the catalytic residues close to productive conformations. A highly conserved surface patch next to the active site was proposed to be the ubiquitin-binding site, a location that is similar to the ubiquitin-binding sites of two other DUBs, Yuh1 and HAUSP [92, 93]. The predicted ubiquitin-binding site on A20 is negatively charged, complementing the positively charged surface of ubiquitin. Biochemical studies showed that A20 OTU removes the entire Lys63-linked polyubiquitin chain from TRAF6, instead of gradually chewing up or internally cleaving the attached polyubiquitin chain, which in turn effectively terminates the NF-κB pathway [90, 91]. The A20 OTU has a broad and open surface surrounding the active site, giving room to accommodate the substrates and the attached polyubiquitin chain [90]. In comparison, Yuh1 has a crossover loop directly over its active site, granting only small or unstructured substrates to access the active site [93].

CYLD

CYLD belongs to the ubiquitin-specific protease (USP)

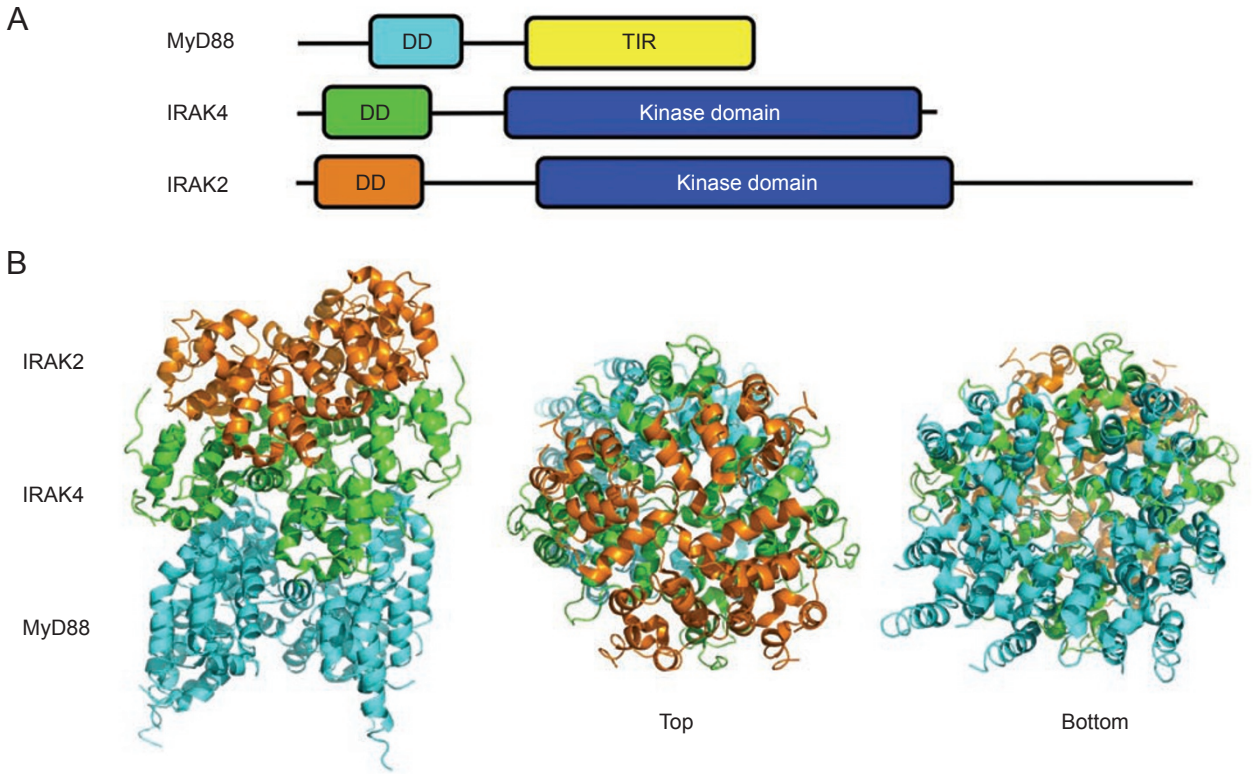

Figure 4 Structure of the MyD88:IRAK4:IRAK2 complex. **(A)** Domain organization of IRAK2, IRAK4 and MyD88. DD: death domain; TIR: Toll/IL-1R homology domain. **(B)** The MyD88:IRAK4:IRAK2 ternary complex structure (PDB:3MOP) with four IRAK2 DD (orange), 4 IRAK4 DD (green) and six MyD88 DD (cyan).

family of DUBs. It contains three cytoskeletal-associated protein-glycine-conserved (CAP-Gly) repeats and one USP domain (Figure 5A). NMR chemical shift perturbation data showed that the third CAP-Gly domain of CYLD directly interacts with a Pro-rich sequence that resides in the C-terminal region of NEMO [94]. Close to the third CAP-Gly is a consensus TRAF2-binding sequence that interacts with the C-terminal TRAF domain of TRAF2 [84]. The USP domain of CYLD is the catalytic unit that mediates disassembly of Lys63-linked polyubiquitin chains. Similar to A20, the USP of CYLD seems to be pre-configured for catalysis even without the bound substrate [95]. The crystal structure of the USP domain of CYLD provides a structural explanation for its specificity toward Lys63-linked polyubiquitin [95] (Figure 5C). This property is attributed to the proximal ubiquitin-binding site near the catalytic site, as Lys63-specific USPs have a different set of conserved residues compared with Lys48-specific USPs. Unlike other USP domains identified so far, CYLD is able to hydrolyze the polyubiquitin chain internally. This makes CYLD more efficient in terms of shutting off the NF-κB pathway. Another special feature about the CYLD USP domain is the presence of an inserted Type I B-box domain that is required for the retention of CYLD protein in the cytosol.

Conclusion

We have come far in terms of understanding the NF-κB pathway. With the structure information, we now have a clearer picture about how NF-κB pathway is regulated. The NF-κB pathway is a classic example of how cells can switch on and switch off an array of genes by tightly regulating one family of transcription factors. Posttranscriptional modifications, proteasome-degradations, translocalizations and oligomerizations are the tricks that cells use to control the flow of the signal transduction. For instance, both destructive and non-destructive ubiquitinations are essential for activation as well as timely shutdown of the NF-κB pathway. Lys63-linked polyubiquitin chains are widely used in the pathway as a platform to recruit and activate downstream molecules. Removal of the Lys63-linked polyubiquitin chains and replacement with the destructive Lys48-linked polyubiquitin chains are ways to efficiently turn off the NF-κB pathway. In addition, there is an emerging

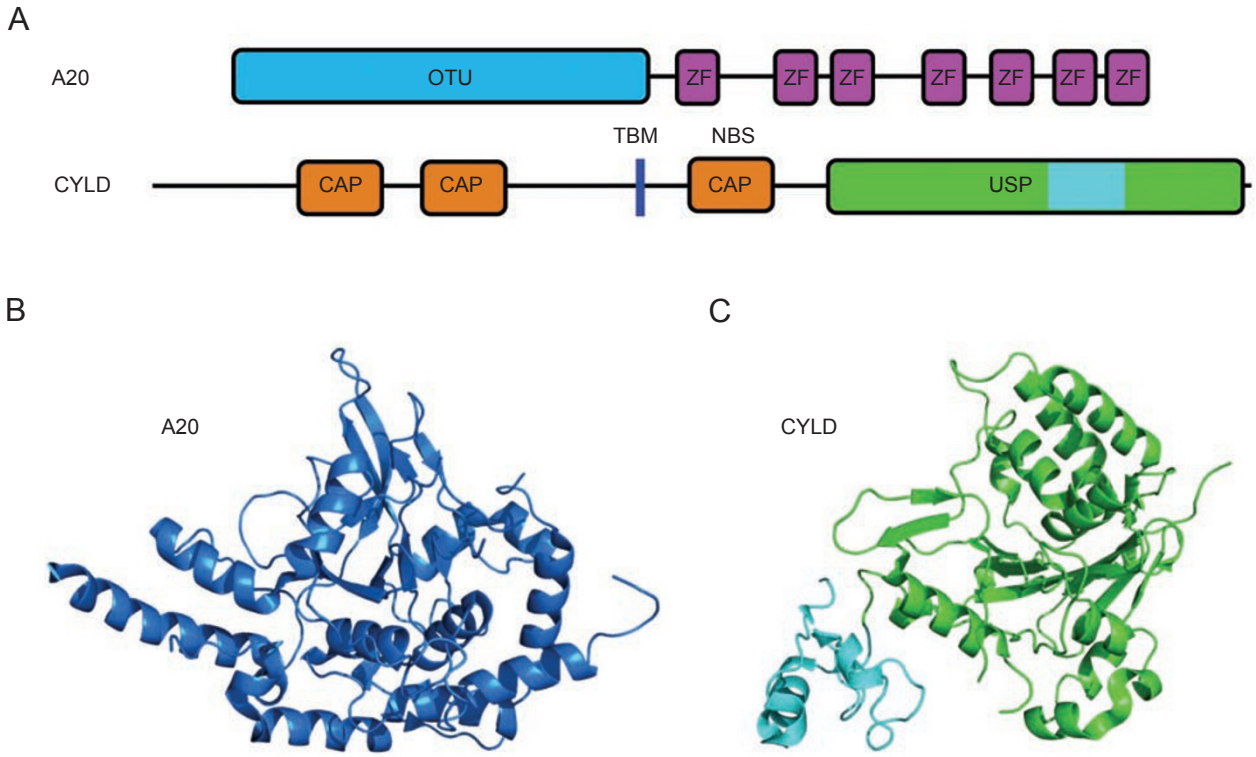

Figure 5 Structures of A20 and CYLD. **(A)** Domain organizations of A20 and CYLD. ZF: zinc finger; CAP: CAP-Gly repeats. **(B)** Structure of A20 OTU domain (PDB:3DKB). **(C)** Structure of the CYLD USP domain (green, 2VHF). The blue bar shows the location of TRAF2-binding motif (TBM, residues 453-PVQES-457). The third CAP-Gly repeat is the NEMO-binding site (NBS). The CYLD USP domain has an inserted Type I B-box domain (cyan).

theme of signaling through oligomerization, which may be previously under-appreciated. Now it is believed that TRAF6 is able to form a higher-order oligomer that is important for downstream signaling. More striking is the "signaling tower" of IRAK2, IRAK4 and MyD88, which is a perfect oligomeric helical structure in the center of a signaling activation platform. Oligomerization may be a great way nature has found to control signaling events, likely in an all-or-none fashion due to the positive cooperativity. While we have come a long way, many questions remain including the central question on how the IKK kinase phosphorylates IκB to activate NF-κB.

Acknowledgments

We apologize to those whose work was not included due to space limitations. The work was supported by NIH grants AI045937, AI050872 and AI079260 (to HW).

References

1 Greten FR, Karin M. The IKK/NF-kappaB activation pathway-a target for prevention and treatment of cancer. *Cancer Lett* 2004; **206**:193-199.
2 Hayden MS, Ghosh S. Signaling to NF-kappaB. *Genes Dev* 2004; **18**:2195-2224.
3 Sen R, Baltimore D. Multiple nuclear factors interact with the immunoglobulin enhancer sequences. *Cell* 1986; **46**:705-716.
4 Gilmore TD, Temin HM. Different localization of the product of the v-rel oncogene in chicken fibroblasts and spleen cells correlates with transformation by REV-T. *Cell* 1986; **44**:791-800.
5 Steward R, Zusman SB, Huang LH, Schedl P. The dorsal protein is distributed in a gradient in early Drosophila embryos. *Cell* 1988; **55**:487-495.
6 Steward R. Dorsal, an embryonic polarity gene in *Drosophila*, is homologous to the vertebrate proto-oncogene, c-rel. *Science* 1987; **238**:692-694.
7 Ghosh S, Gifford AM, Riviere LR, *et al*. Cloning of the p50 DNA binding subunit of NF-kappa B: homology to rel and dorsal. *Cell* 1990; **62**:1019-1029.
8 Kieran M, Blank V, Logeat F, *et al*. The DNA binding subunit of NF-kappa B is identical to factor KBF1 and homologous to the rel oncogene product. *Cell* 1990; **62**:1007-1018.
9 Gilmore TD. Introduction to NF-kappaB: players, pathways, perspectives. *Oncogene* 2006; **25**:6680-6684.
10 Scheidereit C. IkappaB kinase complexes: gateways to NF-kappaB activation and transcription. *Oncogene* 2006; **25**:6685-

6705.
11 Mercurio F, Zhu H, Murray BW, *et al*. IKK-1 and IKK-2: cytokine-activated IkappaB kinases essential for NF-kappaB activation. *Science* 1997; **278**:860-866.
12 Zandi E, Rothwarf DM, Delhase M, Hayakawa M, Karin M. The IkappaB kinase complex (IKK) contains two kinase subunits, IKKalpha and IKKbeta, necessary for IkappaB phosphorylation and NF-kappaB activation. *Cell* 1997; **91**:243-252.
13 DiDonato JA, Hayakawa M, Rothwarf DM, Zandi E, Karin M. A cytokine-responsive IkappaB kinase that activates the transcription factor NF-kappaB. *Nature* 1997; **388**:548-554.
14 Woronicz JD, Gao X, Cao Z, Rothe M, Goeddel DV. IkappaB kinase-beta: NF-kappaB activation and complex formation with IkappaB kinase-alpha and NIK. *Science* 1997; **278**:866-869.
15 Yamaoka S, Courtois G, Bessia C, *et al*. Complementation cloning of NEMO, a component of the IkappaB kinase complex essential for NF-kappaB activation. *Cell* 1998; **93**:1231-1240.
16 Poyet JL, Srinivasula SM, Lin JH, *et al*. Activation of the Ikappa B kinases by RIP via IKKgamma /NEMO-mediated oligomerization. *J Biol Chem* 2000; **275**:37966-37977.
17 Li ZW, Chu W, Hu Y, *et al*. The IKKbeta subunit of IkappaB kinase (IKK) is essential for nuclear factor kappaB activation and prevention of apoptosis. *J Exp Med* 1999; **189**:1839-1845.
18 Tanaka M, Fuentes ME, Yamaguchi K, *et al*. Embryonic lethality, liver degeneration, and impaired NF-kappa B activation in IKK-beta-deficient mice. *Immunity* 1999; **10**:421-429.
19 Senftleben U, Cao Y, Xiao G, *et al*. Activation by IKKalpha of a second, evolutionary conserved, NF-kappa B signaling pathway. *Science* 2001; **293**:1495-1499.
20 Hu Y, Baud V, Delhase M, *et al*. Abnormal morphogenesis but intact IKK activation in mice lacking the IKKalpha subunit of IkappaB kinase. *Science* 1999; **284**:316-320.
21 Chen ZJ. Ubiquitin signalling in the NF-kappaB pathway. *Nat Cell Biol* 2005; **7**:758-765.
22 Mahoney DJ, Cheung HH, Mrad RL, *et al*. Both cIAP1 and cIAP2 regulate TNFalpha-mediated NF-kappaB activation. *Proc Natl Acad Sci USA* 2008; **105**:11778-11783.
23 Vince JE, Pantaki D, Feltham R, *et al*. TRAF2 must bind to cellular inhibitors of apoptosis for tumor necrosis factor (tnf) to efficiently activate nf-{kappa}b and to prevent tnf-induced apoptosis. *J Biol Chem* 2009; **284**:35906-35915.
24 Wu CJ, Conze DB, Li T, Srinivasula SM, Ashwell JD. Sensing of Lys 63-linked polyubiquitination by NEMO is a key event in NF-kappaB activation [corrected]. *Nat Cell Biol* 2006; **8**:398-406.
25 Ea CK, Deng L, Xia ZP, Pineda G, Chen ZJ. Activation of IKK by TNFalpha requires site-specific ubiquitination of RIP1 and polyubiquitin binding by NEMO. *Mol Cell* 2006; **22**:245-257.
26 Zarnegar BJ, Wang Y, Mahoney DJ, *et al*. Noncanonical NF-kappaB activation requires coordinated assembly of a regulatory complex of the adaptors cIAP1, cIAP2, TRAF2 and TRAF3 and the kinase NIK. *Nat Immunol* 2008; **9**:1371-1378.
27 Vince JE, Wong WW, Khan N, *et al*. IAP antagonists target cIAP1 to induce TNFalpha-dependent apoptosis. *Cell* 2007; **131**:682-693.
28 Varfolomeev E, Blankenship JW, Wayson SM, *et al*. IAP antagonists induce autoubiquitination of c-IAPs, NF-kappaB activation, and TNFalpha-dependent apoptosis. *Cell* 2007; **131**:669-681.
29 Petersen SL, Wang L, Yalcin-Chin A, *et al*. Autocrine TNFalpha signaling renders human cancer cells susceptible to Smac-mimetic-induced apoptosis. Cancer *Cell* 2007; **12**:445-456.
30 Vallabhapurapu S, Matsuzawa A, Zhang W, *et al*. Nonredundant and complementary functions of TRAF2 and TRAF3 in a ubiquitination cascade that activates NIK-dependent alternative NF-kappaB signaling. *Nat Immunol* 2008; **9**:1364-1370.
31 Wu H, Tschopp J, Lin SC. Smac mimetics and TNFalpha: a dangerous liaison? *Cell* 2007; **131**:655-658.
32 Biswas DK, Shi Q, Baily S, *et al*. NF-kappa B activation in human breast cancer specimens and its role in cell proliferation and apoptosis. *Proc Natl Acad Sci USA* 2004; **101**:10137-10142.
33 Greten FR, Eckmann L, Greten TF, *et al*. IKKbeta links inflammation and tumorigenesis in a mouse model of colitis-associated cancer. *Cell* 2004; **118**:285-296.
34 Davis RE, Brown KD, Siebenlist U, Staudt LM. Constitutive nuclear factor kappaB activity is required for survival of activated B cell-like diffuse large B cell lymphoma cells. *J Exp Med* 2001; **194**:1861-1874.
35 Zhou Y, Eppenberger-Castori S, Marx C, *et al*. Activation of nuclear factor-kappaB (NFkappaB) identifies a high-risk subset of hormone-dependent breast cancers. *Int J Biochem Cell Biol* 2005; **37**:1130-1144.
36 Andresen L, Jorgensen VL, Perner A, *et al*. Activation of nuclear factor {kappa}B in colonic mucosa from patients with collagenous and ulcerative colitis. *Gut* 2005; **54**:503-509.
37 Shukla S, Maclennan GT, Marengo SR, Resnick MI, Gupta S. Constitutive activation of PI3K-Akt and NF-kappaB during prostate cancer progression in autochthonous transgenic mouse model. *Prostate* 2005; **64**:224-239.
38 Krappmann D, Emmerich F, Kordes U, *et al*. Molecular mechanisms of constitutive NF-kappaB/Rel activation in Hodgkin/Reed-Sternberg cells. *Oncogene* 1999; **18**:943-953.
39 Aupperle K, Bennett B, Han Z, *et al*. NF-kappa B regulation by I kappa B kinase-2 in rheumatoid arthritis synoviocytes. *J Immunol* 2001; **166**:2705-2711.
40 Ludwig L, Kessler H, Wagner M, *et al*. Nuclear factor-kappaB is constitutively active in C-cell carcinoma and required for RET-induced transformation. *Cancer Res* 2001; **61**:4526-4535.
41 Tamatani T, Azuma M, Aota K, *et al*. Enhanced IkappaB kinase activity is responsible for the augmented activity of NF-kappaB in human head and neck carcinoma cells. *Cancer Lett* 2001; **171**:165-172.
42 Baeuerle PA, Henkel T. Function and activation of NF-kappa B in the immune system. *Annu Rev Immunol* 1994; **12**:141-179.
43 Blank V, Kourilsky P, Israel A. NF-kappa B and related proteins: Rel/dorsal homologies meet ankyrin-like repeats. *Trends Biochem Sci* 1992; **17**:135-140.
44 Chen FE, Ghosh G. Regulation of DNA binding by Rel/NF-kappaB transcription factors: structural views. *Oncogene* 1999; **18**:6845-6852.
45 Ghosh G, van Duyne G, Ghosh S, Sigler PB. Structure of NF-kappa B p50 homodimer bound to a kappa B site. *Nature* 1995; **373**:303-310.

46 Muller CW, Rey FA, Sodeoka M, Verdine GL, Harrison SC. Structure of the NF-kappa B p50 homodimer bound to DNA. *Nature* 1995; **373**:311-317.
47 Chen FE, Huang DB, Chen YQ, Ghosh G. Crystal structure of p50/p65 heterodimer of transcription factor NF-kappaB bound to DNA. *Nature* 1998; **391**:410-413.
48 Chen YQ, Ghosh S, Ghosh G. A novel DNA recognition mode by the NF-kappa B p65 homodimer. *Nat Struct Biol* 1998; **5**:67-73.
49 Cramer P, Larson CJ, Verdine GL, Muller CW. Structure of the human NF-kappaB p52 homodimer-DNA complex at 2.1 A resolution. *EMBO J* 1997; **16**:7078-7090.
50 Huxford T, Ghosh G. A structural guide to proteins of the NF-kappaB signaling module. *Cold Spring Harb Perspect Biol* 2009; **1**:a000075.
51 Michel F, Soler-Lopez M, Petosa C, *et al*. Crystal structure of the ankyrin repeat domain of Bcl-3: a unique member of the IkappaB protein family. *EMBO J* 2001; **20**:6180-6190.
52 Huxford T, Huang DB, Malek S, Ghosh G. The crystal structure of the IkappaBalpha/NF-kappaB complex reveals mechanisms of NF-kappaB inactivation. *Cell* 1998; **95**:759-770.
53 Jacobs MD, Harrison SC. Structure of an IkappaBalpha/NF-kappaB complex. *Cell* 1998; **95**:749-758.
54 Malek S, Huang DB, Huxford T, Ghosh S, Ghosh G. X-ray crystal structure of an IkappaBbeta x NF-kappaB p65 homodimer complex. *J Biol Chem* 2003; **278**:23094-23100.
55 Rothwarf DM, Zandi E, Natoli G, Karin M. IKK-gamma is an essential regulatory subunit of the IkappaB kinase complex. *Nature* 1998; **395**:297-300.
56 Mercurio F, Murray BW, Shevchenko A, *et al*. IkappaB kinase (IKK)-associated protein 1, a common component of the heterogeneous IKK complex. *Mol Cell Biol* 1999; **19**:1526-1538.
57 Rushe M, Silvian L, Bixler S, *et al*. Structure of a NEMO/IKK-associating domain reveals architecture of the interaction site. *Structure* 2008; **16**:798-808.
58 May MJ, D'Acquisto F, Madge LA, *et al*. Selective inhibition of NF-kappaB activation by a peptide that blocks the interaction of NEMO with the IkappaB kinase complex. *Science* 2000; **289**:1550-1554.
59 Lo YC, Maddineni U, Chung JY, *et al*. High-affinity interaction between IKKbeta and NEMO. *Biochemistry* 2008; **47**:3109-3116.
60 Bagneris C, Ageichik AV, Cronin N, *et al*. Crystal structure of a vFlip-IKKgamma complex: insights into viral activation of the IKK signalosome. *Mol Cell* 2008; **30**:620-631.
61 Lo YC, Lin SC, Rospigliosi CC, *et al*. Structural Basis for Recognition of Diubiquitins by NEMO. *Mol Cell* 2009; **33**:602-615.
62 Yoshikawa A, Sato Y, Yamashita M, *et al*. Crystal structure of the NEMO ubiquitin-binding domain in complex with Lys 63-linked di-ubiquitin. *FEBS Lett* 2009; **583**:3317-3322.
63 Cordier F, Grubisha O, Traincard F, *et al*. The zinc finger of NEMO is a functional ubiquitin-binding domain. *J Biol Chem* 2009; **284**:2902-2907.
64 Cordier F, Vinolo E, Veron M, Delepierre M, Agou F. Solution structure of NEMO zinc finger and impact of an anhidrotic ectodermal dysplasia with immunodeficiency-related point mutation. *J Mol Biol* 2008; **377**:1419-1432.
65 Banner DW, D'Arcy A, Janes W, *et al*. Crystal structure of the soluble human 55 kd TNF receptor-human TNF beta complex: implications for TNF receptor activation. *Cell* 1993; **73**:431-445.
66 Park YC, Burkitt V, Villa AR, Tong L, Wu H. Structural basis for self-association and receptor recognition of human TRAF2. *Nature* 1999; **398**:533-538.
67 Ye H, Park YC, Kreishman M, Kieff E, Wu H. The structural basis for the recognition of diverse receptor sequences by TRAF2. *Mol Cell* 1999; **4**:321-330.
68 Park YC, Ye H, Hsia C, *et al*. A novel mechanism of TRAF signaling revealed by structural and functional analyses of the TRADD-TRAF2 interaction. *Cell* 2000; **101**:777-787.
69 Ye H, Arron JR, Lamothe B, *et al*. Distinct molecular mechanism for initiating TRAF6 signalling. *Nature* 2002; **418**:443-447.
70 Ye H, Cirilli M, Wu H. The use of construct variation and diffraction data analysis in the crystallization of the TRAF domain of human tumor necrosis factor receptor associated factor 6. *Acta Crystallogr D Biol Crystallogr* 2002; **58**:1886-1888.
71 Ye H, Wu H. Thermodynamic characterization of the interaction between TRAF2 and receptor peptides by isothermal titration calorimetry. *Proc Natl Acad Sci USA* 2000; **97**:8961-8966.
72 Ni CZ, Welsh K, Leo E, *et al*. Molecular basis for CD40 signaling mediated by TRAF3. *Proc Natl Acad Sci USA* 2000; **97**:10395-10399.
73 Guasparri I, Wu H, Cesarman E. The KSHV oncoprotein vFLIP contains a TRAF-interacting motif and requires TRAF2 and TRAF3 for signalling. *EMBO Rep* 2006; **7**:114-119.
74 Yin Q, Lin SC, Lamothe B, *et al*. E2 interaction and dimerization in the crystal structure of TRAF6. *Nat Struct Mol Biol* 2009; **16**:658-666.
75 Yin Q, Lamothe B, Darnay BG, Wu H. Structural Basis for the Lack of E2 Interaction in the RING Domain of TRAF2. *Biochemistry* 2009; **48**:10558-67.
76 Zheng C, Kabaleeswaran V, Wang Y, Cheng G, Wu H. Crystal structures of the TRAF2: cIAP2 and the TRAF1: TRAF2: cIAP2 complexes: affinity, specificity, and regulation. *Mol Cell* 2010; **38**:101-113.
77 Mace PD, Smits C, Vaux DL, Silke J, Day CL. Asymmetric recruitment of cIAPs by TRAF2. *J Mol Biol* 2010; **400**:8-15.
78 Varfolomeev E, Goncharov T, Fedorova AV, *et al*. c-IAP1 and c-IAP2 are critical mediators of tumor necrosis factor alpha (TNFalpha)-induced NF-kappaB activation. *J Biol Chem* 2008; **283**:24295-24299.
79 Lin SC, Lo YC, Wu H. Helical assembly in the MyD88-IRAK4-IRAK2 complex in TLR/IL-1R signalling. *Nature* 2010; **465**:885-890.
80 Dai Y, Lawrence TS, Xu L. Overcoming cancer therapy resistance by targeting inhibitors of apoptosis proteins and nuclear factor-kappa B. *Am J Transl Res* 2009; **1**:1-15.
81 Lin Y, Bai L, Chen W, Xu S. The NF-kappaB activation pathways, emerging molecular targets for cancer prevention and therapy. *Expert Opin Ther Targets*; **14**:45-55.
82 Hymowitz SG, Wertz IE. A20: from ubiquitin editing to tumour suppression. *Nat Rev Cancer*; **10**:332-341.
83 Krikos A, Laherty CD, Dixit VM. Transcriptional activation of the tumor necrosis factor alpha-inducible zinc finger protein, A20, is mediated by kappa B elements. *J Biol Chem* 1992; **267**:17971-17976.

84 Kovalenko A, Chable-Bessia C, Cantarella G, *et al*. The tumour suppressor CYLD negatively regulates NF-kappaB signalling by deubiquitination. *Nature* 2003; **424**:801-805.
85 Trompouki E, Hatzivassiliou E, Tsichritzis T, *et al*. CYLD is a deubiquitinating enzyme that negatively regulates NF-kappaB activation by TNFR family members. *Nature* 2003; **424**:793-796.
86 Brummelkamp TR, Nijman SM, Dirac AM, Bernards R. Loss of the cylindromatosis tumour suppressor inhibits apoptosis by activating NF-kappaB. *Nature* 2003; **424**:797-801.
87 Makarova KS, Aravind L, Koonin EV. A novel superfamily of predicted cysteine proteases from eukaryotes, viruses and Chlamydia pneumoniae. *Trends Biochem Sci* 2000; **25**:50-52.
88 Wertz IE, O'Rourke KM, Zhou H, *et al*. De-ubiquitination and ubiquitin ligase domains of A20 downregulate NF-kappaB signalling. *Nature* 2004; **430**:694-699.
89 Heyninck K, Beyaert R. A20 inhibits NF-kappaB activation by dual ubiquitin-editing functions. *Trends Biochem Sci* 2005; **30**:1-4.
90 Lin SC, Chung JY, Lamothe B, *et al*. Molecular basis for the unique deubiquitinating activity of the NF-kappaB inhibitor A20. *J Mol Biol* 2008; **376**:526-540.
91 Komander D, Barford D. Structure of the A20 OTU domain and mechanistic insights into deubiquitination. *Biochem J* 2008; **409**:77-85.
92 Hu M, Li P, Li M, *et al*. Crystal structure of a UBP-family deubiquitinating enzyme in isolation and in complex with ubiquitin aldehyde. *Cell* 2002; **111**:1041-1054.
93 Johnston SC, Riddle SM, Cohen RE, Hill CP. Structural basis for the specificity of ubiquitin C-terminal hydrolases. *EMBO J* 1999; **18**:3877-3887.
94 Saito K, Kigawa T, Koshiba S, *et al*. The CAP-Gly domain of CYLD associates with the proline-rich sequence in NEMO/IKKgamma. *Structure* 2004; **12**:1719-1728.
95 Komander D, Lord CJ, Scheel H, *et al*. The structure of the CYLD USP domain explains its specificity for Lys63-linked polyubiquitin and reveals a B box module. *Mol Cell* 2008; **29**:451-464.